Research Article

TOF-SIMS Investigation on Nuclear Transmutation from Sr to Mo with Deuterium Permeation through Multi-layered Pd/CaO

A. Murase *, N. Takahashi, S. Hibi, T. Hioki and T. Motohiro

Toyota Central R & D Laboratories Inc., Nagakute, Aichi 480-1192, Japan

J. Kasagi

Research Center for Electron Photon Science, Tohoku University, Sendai 982-0826, Japan

Abstract

The selective nuclear transmutation from ^{88}Sr to ^{96}Mo reported by Iwamura et al. was investigated replacing electrochemical deposition with ion implantation for seeding ^{88}Sr$^+$ and replacing a quadrupole mass spectrometer with a time of flight mass spectrometer for secondary ion mass spectrometry (TOF-SIMS) for analysis of possible transmuted products. At the surface of the Sr implanted Pd/CaO multilayer foil, Mo was clearly detected by X-ray photoelectron spectroscopy (XPS) after deuterium gas permeation. After the D$_2$ permeation, the sample was heat treated in the air to remove S which condensed at the surface during the permeation. After the successful removal of S, Mo could be clearly detected by XPS on the surface of the ^{88}Sr$^+$ implanted Pd/CaO multilayer foil. The isotopic abundance ratio of the surface Mo measured by TOF-SIMS was similar to that of natural Mo. However, after the removal of the outermost surface layer with ion sputtering, the observed isotopic abundance ratio of Mo changed from that of natural Mo with an isolatedly strong peak at a mass close to ^{96}Mo. This result duly suggests that the transmutation from ^{88}Sr to ^{96}Mo had took place, although the peak of $m/z = 96$ might be also assigned to GaAl$^+$, Ca$_2$O$^+$ or CaFe$^+$, beside ^{96}Mo$^+$. By further analyses of the TOF-SIMS data from the viewpoint of accurate masses, depth profiles and isotopic abundances, it was clarified that the peak of $m/z = 96$ was assigned to Ca$_2$O$^+$ originated from Pd/CaO multilayer.
© 2012 ISCMNS. All rights reserved.

Keywords: Deuterium permeation, Pd/CaO multilayer, Time of flight secondary ion mass spectrometry, Transmutation, X-ray photoelectron spectroscopy

1. Introduction

Nuclear transmutation with deuterium (D$_2$) gas permeation through a Pd/CaO multilayer foil has firstly been reported by Iwamura et al. [1]. Identifying the surface elements on the Pd foil covered with (Pd/CaO)$_n$ multilayer film before and after the D$_2$ gas permeation over one week at a temperature as low as 343 K, they have given the evidences that

---

*E-mail: e0483@mosk.tytlabs.co.jp

electrochemically deposited Sr and Cs change to Mo and Pr, respectively. The isotopic abundance ratio for the induced Mo was quite different from that for natural Mo: this observation with secondary ion mass spectrometry by a quadrupole mass spectrometer has suggested that the change is caused by a nuclear process. By the D_2 gas permeation method, they have further found that Ba changes to Sm [2].

It is considered that these results are easily replicated in different laboratories. However, only a limited number of replication experiments have been reported so far [3–5]. One of the difficulties is to reproduce a condition of the high D_2 gas flow rate [6]. A D_2 gas flow rate through Pd is sensitive to the state of the surface. Therefore, appropriate pretreatments of Pd as well as clean experimental environment are required to realize a high D_2 flow rate. We have reported that commercially available Pd foils are often contaminated with S and a segregation of the S impurity on the surface during D_2 gas permeation results in a lowering of the flow rate [7–9]. Furthermore, if S is on the surface, it is difficult to examine the generation of Mo using X-ray photoelectron spectroscopy (XPS), because a S2s peak in the XPS spectrum overlaps with Mo 3d peaks [7]. In our previous paper, we reported that a small amount of S impurity in Pd concentrates and forms sulfuric compounds at the surface during D_2 permeation and the sulfuric compounds are removed by annealing in air at 1273 K for 10 min after the permeation [8,9].

The selective nuclear transmutation from ^{88}Sr to ^{96}Mo reported by Iwamura et al. has been investigated replacing electrochemical deposition with ion implantation for seeding ^{88}Sr$^+$ without an implantation of any other isotopes and replacing a quadrupole mass spectrometer with a time of flight mass spectrometer for secondary ion mass spectrometry (TOF-SIMS), which has a great advantage in mass resolution, for analysis of possible transmuted products [9]. In this study, a more detailed TOF-SIMS study has been made in order to clarify the origin of the anomalous isotopic abundance ratio for the induced Mo. Pd foils with five sets of Pd/CaO layers were implanted with 65-keV ^{88}Sr$^+$ ions, and were subjected to D_2 gas permeation treatment at 343 K same as Iwamura's report [1]. XPS and TOF-SIMS measurements were performed to examine the change of surface elements before and after the gas permeation. This paper reports the results of the TOF-SIMS investigation from the view point of accurate masses, isotope abundances and depth profiles on nuclear transmutation from Sr to Mo.

2. Experimental

2.1. Sample preparation

Pd foils of 50 μm (purity: 99.97%) in thickness were commercially obtained from the Nilaco Corporation. The as-purchased foils were first ultrasonically cleaned with ethanol and heat-treated in vacuum (5×10^{-5} Pa) at 1223 K for 5 h and subsequently in air at 873 K for 10 min. Layers of CaO and Pd were piled up alternately on the substrate Pd foils by the RF sputter deposition method. The structure of the multilayer was the same as reported by Iwamura et al.: Pd (40 nm) / CaO (2 nm)/ Pd (18 nm)/ CaO (2 nm)/ Pd (18 nm)/ CaO (2 nm)/ Pd (18 nm)/ CaO (2 nm)/ Pd (18 nm)/ CaO (2 nm)/ Pd foil (50 μm). Then ^{88}Sr$^+$ was implanted in the multilayer foil at 65 keV and a dose of 1×10^{16} ions/cm^2. Subsequently the foils were heat-treated in the air at 573 K for 10 min in order to remove carbonaceous materials deposited during the ion implantation. The samples were then subjected to D_2 gas permeation treatments at 343 K for about 10 days. The D_2 permeation system was the same with that reported by us previously [7,8,10]. The upstream side was filled with D_2 of 200 kPa. The purity of the D_2 gas was 99.995%. The downstream side was evacuated with a dry pump and a turbo molecular pump. The upstream side was connected with a reservoir tank of 1.0 L. The flow rate of D_2 was determined from the reduction of the pressure of the tank. A metal O-ring was used for the vacuum seal. An example of the relationship between permeation rate and time is shown in Fig. 1. After the permeation, the samples were annealed in the air at 1273 K for 10 min, in order to remove S, which had concentrated at the surface during D_2 permeation and disturbs the detection of Mo by XPS. The origin of the S contamination and the details of above procedure for removing the influences of S are described in a separate paper [11].
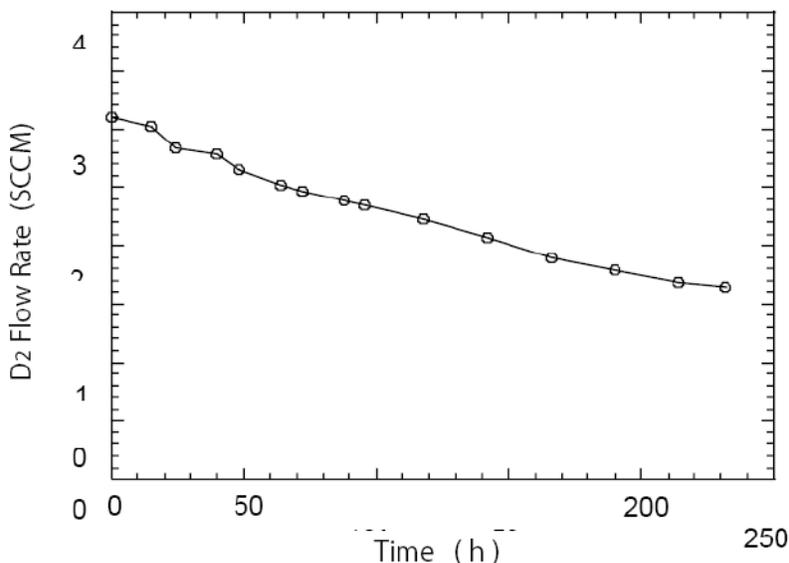
Figure 1. Variation of permeation rate with time for a ^{88}Sr$^+$ implanted Pd/CaO multilayer sample.

2.2. Analysis

XPS measurements were performed with ULVAC-PHI Inc. "Quantera SXM" (20 kV, 100 W): the X-ray used for excitation of photoelectrons was the monochromatic Al–Kα line (1.438 keV). The size of the incident X-ray beam was 100×1500 μm^2 on the sample.

TOF-SIMS measurements were performed with ULVAC-PHI Inc. "TRIFT II" instrument. High mass resolution spectra of $M/\Delta M > 5000$ at m/z 27 (C$_2$H$_3^+$) were acquired using pulsed ^{69}Ga$^+$ ion beam with an impact energy of 15 keV, an ion current of 2 nA for one pulse, a pulse width of 13 ns (700 ps after bunching) and a pulse frequency of 10 kHz. Total ion doses in these measurements were $< 1 \times 10^{12}$ ions/cm^2. For the depth profiling with TOF-SIMS, continuous ^{69}Ga$^+$ ion beam with impact energy of 15 keV was used for sputtering. The sputtering area was 300×300 μm^2, and the sputter rate was approximately 0.4 nm/60 s in the case of the (111) surface of crystal silicon.

3. Results and Discussion

3.1. XPS spectrum of surface after annealing in air

The XPS spectrum around Mo3d for a ^{88}Sr$^+$ implanted Pd/CaO multilayer sample after D$_2$ permeation is shown in Fig. 2. This sample maintained a comparatively high permeation rate of 1.6 SCCM even at the permeation time of 230 h as shown in Fig. 1. The two peaks in the spectrum definitely correspond to Mo3d5/2 and Mo3d3/2, because (i) the intensity ratio is 3:2 and (ii) the energy difference between the two peaks is 3.13 eV. This spectrum was obtained when the sample was annealed in the air after the D$_2$ permeation treatment. The air annealing was conducted in order to remove S accumulated onto the surface of the sample during the D$_2$ permeation treatment. The influences of S on the permeation rate and elemental analysis with XPS are described in [10]. Then, TOF-SIMS analyses were performed
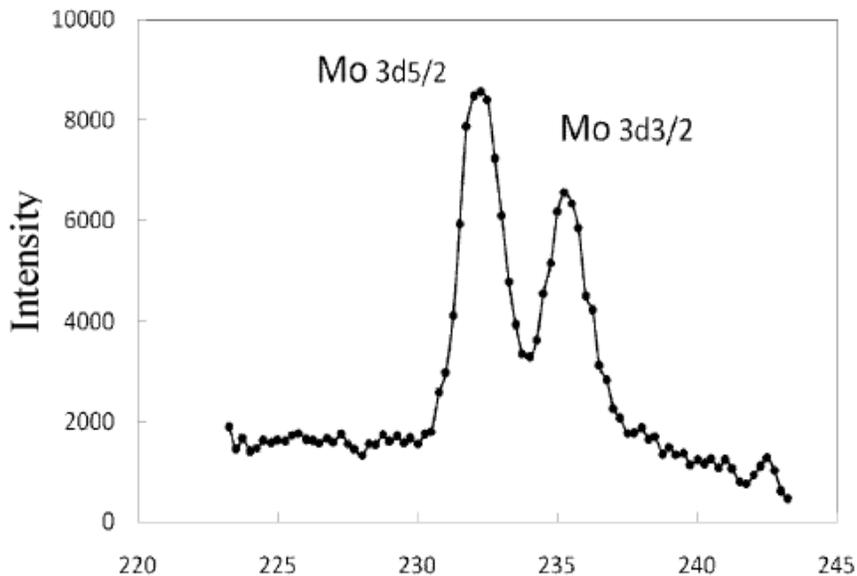
Figure 2. XPS spectrum around Mo_{3d} for $^{88}Sr^+$ implanted Pd/CaO multilayer sample after D_2 permeation followed by annealing in the air.

in order to clarify the origin of this Mo.

3.2. TOF-SIMS spectra of surfaces and sputtered surfaces

Figure 3 shows TOF-SIMS spectra of the Sr implanted Pd/CaO multilayer after D_2 permeation. On the surface, the existence of ^{88}Sr is confirmed by a peak of $m/z = 88$ in Fig. 3(a) and all the isotopes of natural Mo appear as shown in Fig. 3(b). The spectrum after removing an outermost surface layer by ion sputtering for 60 s (about 0.4 nm in depth), however, a stronger peak is observed at the mass of ^{96}Mo than peaks of other Mo isotopes as is shown in Fig. 3(c). This spectrum is similar to that reported by Iwamura et al. [1], suggesting the evidence of the transmutation from ^{88}Sr to ^{96}Mo.

Figure 4 shows the spectra before D_2 permeation. They were taken for the area where Sr^+ ions had not been implanted. On the surface, neither Sr nor Mo isotopes are observed as shown in Figs. 4(a) and (b), respectively. However, when the outermost surface layer is removed by sputtering for 60 s, a peak at a mass close to ^{96}Mo is observed as shown in Fig. 4(c). The peak cannot be due to ^{96}Mo of nature, because any other Mo isotopes, especially the most abundant ^{98}Mo, are not seen. This result indicates that the peak at a mass closed to ^{96}Mo observed by TOF-SIMS after removing the outermost surface layer is not the ^{96}Mo generated by transmutation from ^{88}Sr. This peak was observed from all of the 60s sputtered surfaces of Pd/CaO multilayer samples before and after D_2 permeation. We refer to this peak as ^{96}X, here. Candidate materials for X are GaAl, Ca_2O and CaFe besides ^{96}Mo as shown in Table 1. Then, we attempted to narrow the possibilities of the candidates from accurate mass, isotope abundance and depth profiles obtained by TOF-SIMS measurements.

Table 1. Candidates for X.

| Molecule	Mass	Source material
Ca_2O	95.920	Pd/CaO multilayer
GaAl	95.907	Ga: $^{69}Ga^+$ primary ion for TOF-SIMS Al: impurity in Pd
CaFe	95.898	Ca: Pd/CaO multilayer Fe: impurity in Pd
^{96}Mo	95.905	

3.3. Accurate mass

The accurate mass of peaks at $m/z = 96$ read off from the spectra of Figs. 3(b), (c) and 4(c), and the deviation of each accurate mass from the mass of GaAl, Ca_2O, CaFe and ^{96}Mo are shown in Table 2. In this case, all the spectra were calibrated with the same ions; CH^+, $C_2H_3^+$, $C_3H_5^+$, $^{40}Ca^+$ and $^{69}Ga^+$. The peak of $m/z = 96$ observed from the surface after D_2 permeation (Fig. 3(b)) can be assigned to $^{96}Mo^+$ originating from natural Mo because of its isotope abundance. On the other hand, the masses of the $^{96}X^+$ observed from sputtered surfaces both before (Fig. 4(c)) and after (Fig. 3(c)) D_2 permeation are shifting from that (Fig. 3(b)) of the surface after D_2 permeation and are rather closer to the mass of Ca_2O than to the mass of ^{96}Mo and GaAl. And this shift of mass with sputtering indicates that the $^{96}X^+$ observed on the sputtered surfaces cannot be assigned to $^{96}Mo^+$. CaFe is still less corresponding than other candidates. From these results, the highest possibility for the assignment of ^{96}X is considered to be Ca_2O among the candidates of ^{96}X listed in Tables 1 and 2.

3.4. Isotope abundance

Among the candidates of ^{96}X, Ca_2O has an isotope peak of $^{44}Ca^{40}CaO$ at $m/z = 99.9$ beside the main peak of $^{40}Ca_2O$ at $m/z = 95.9$, and the ratio of the peak intensity of $m/z = 99.9$ to that of $m/z = 95.92$ is approximately 1–25. From
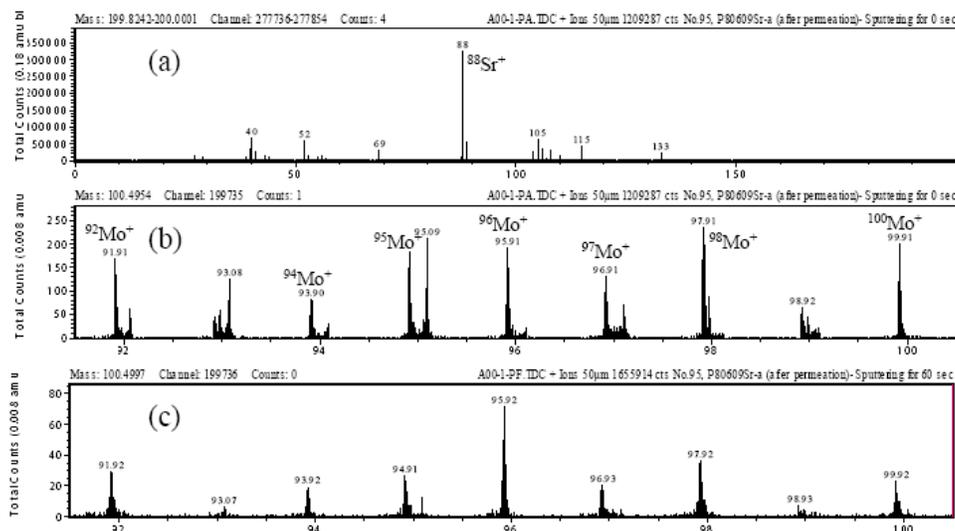
Figure 3. TOF-SIMS spectra for Sr implanted Pd/CaO multilayer after D_2 permeation; (a) spectrum in wide mass range at surface; (b) spectrum around Mo at surface; (c) spectrum around Mo after sputtering for 60 s.
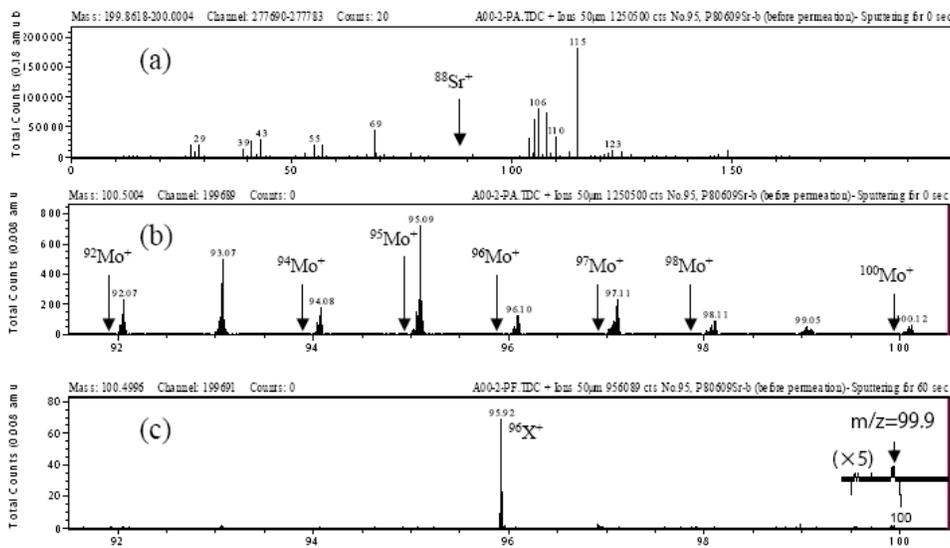
Figure 4. TOF-SIMS spectra for Pd/CaO multilayer (un-implanted area) before D_2 permeation; (a) spectrum in wide mass range at surface; (b) spectrum around Mo at surface; (c) spectrum around Mo after sputtering for 60 s.
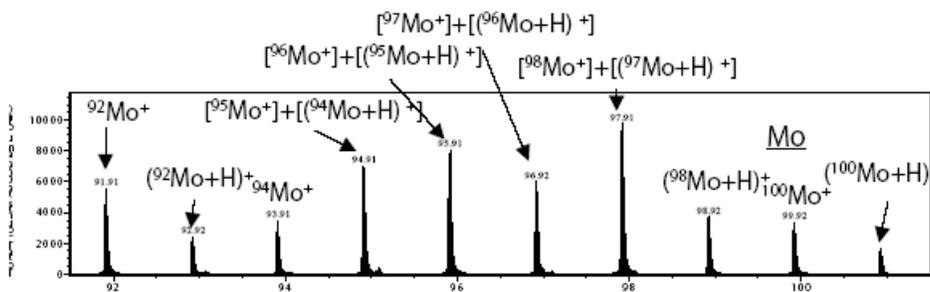
Figure 5. TOF-SIMS spectrum of the surface of Mo metal plate, and assignment of each peak.

Table 2. Accurate mass of the peak at $m/z = 95.9$ for each spectrum, and deviation from the theoretical mass of each candidate for ^{96}X.

Spectrum	Accurate mass (measured)	Deviation from the mass of each candidate			
		Ca_2O	GaAl	CaFe	^{96}Mo
Figure 3(b)	95.909	0.011	0.002	0.011	0.004
Figure 3(c)	95.916	0.004	0.014	0.018	0.011
Figure 4(c)	95.916	0.004	0.014	0.018	0.011
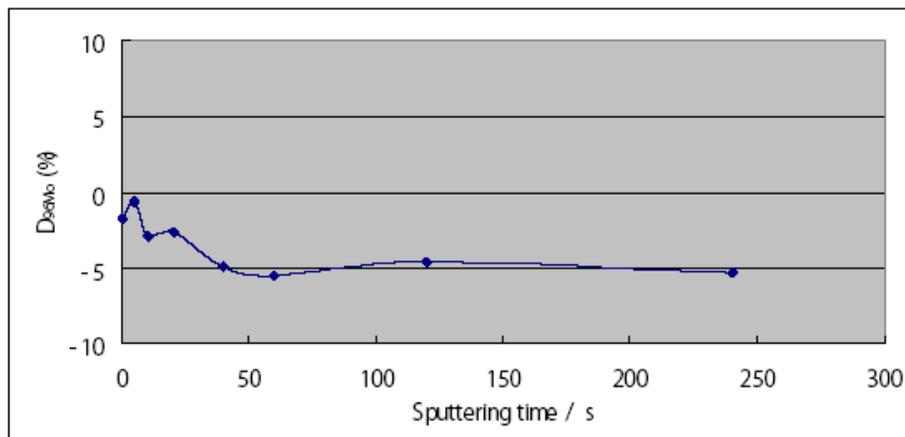
Figure 6.   Relationship between deviations of measured intensities from theoretical intensity for $^{96}Mo^+$ calculated with Eq. (3) and sputtering time.

Fig. 4(c), a peak at $m/z = 99.9$ is observed. From Fig. 3(c), on the other hand, many peaks of natural Mo isotopes disturb the confirmation of the peak of $^{44}Ca^{40}CaO$. Therefore, Ca_2O is not negative for the candidate of ^{96}X.

On the other hand, ^{96}Mo or GaAl has no isotope ion. Therefore, the possibility of these for the candidates of ^{96}X cannot be evaluated by isotope abundance.

CaFe which was negative from accurate mass has an isotope of $Ca^{54}Fe$ at $m/z = 93.9$ beside the main peak of $Ca^{56}Fe$ at $m/z = 95.90$, and the ratio of the peak intensity of $m/z = 93.9$ to that of $m/z = 95.9$ is approximately 1–16. From Fig. 4(c), however, no peak at $m/z = 93.9$ is observed. Therefore, the possibility of CaFe is denied for the candidate of ^{96}X also from isotope abundance.

3.5. Depth profiles

By the evaluation with accurate mass and isotope abundance, as mentioned above, it was found that Ca_2O is the most probable for the candidate of ^{96}X and that ^{96}Mo or CaFe is negative. However, GaAl has not been completely denied yet, although its probability for the candidate of ^{96}X is lower than that of Ca_2O. Then, further investigation for the possibilities of these candidates was attempted by comparing the depth profiles of ions relating to the candidates. For this investigation, it is necessary to divide the peak of $m/z = 95.9$ on measured spectra into $^{96}X^+$ and $^{96}Mo^+$ of nature. For this purpose, the reliability of the peak intensity of $^{96}Mo^+$ of nature calculated from measured data was evaluated by comparing it with theoretical intensity of $^{96}Mo^+$ calculated from natural abundance and measured intensity as follows;

The peak intensity of $m/z = 95.9$ measured from a TOF-SIMS spectrum of a surface of natural Mo is not the intensity of $^{96}Mo^+$, because it consists of $^{96}Mo^+$ and $(^{95}Mo+H)^+$, as shown in Fig. 5. Among the observed peaks, the measured peak intensities of $m/z = 91.9, m/z = 92.9, m/z = 93.9, m/z = 98.9, m/z = 99.9$, and $m/z = 100.9$ are those of $^{92}Mo^+, (^{92}Mo+H)^+, ^{94}Mo^+, (^{98}Mo+H)^+, ^{100}Mo^+$, and $(^{100}Mo+H)^+$, respectively. Therefore, the ratio of intensities of (Mo+H) to Mo can be calculated from the ratio of peak intensities of $m/z = 92.9$ and $m/z = 91.9$, or $m/z = 109.9$ and $m/z = 99.9$. In this study, the ratio of Mo+H to Mo was calculated by the measured peak intensities of $m/z = 92.9$ and $m/z = 91.9$. By this ratio, the intensity of $^{96}Mo^+$ (I_{96Mo}) can be calculated from measured peak

intensities as Eq. (1).

$$
\begin{aligned}
I_{96\text{Mo}} &= I_{95.9} - I_{(95\text{Mo}+\text{H})} \\
&= I_{95.9} - (I_{92.9}/I_{91.9})I_{95\text{Mo}} \\
&= I_{95.9} - (I_{92.9}/I_{91.9})[I_{94.9} - (I_{92.9}/I_{91.9})I_{93.9}],
\end{aligned} \tag{1}
$$

where, $I_{95.9}$, $I_{92.9}$, $I_{91.9}$, $I_{94.9}$, and $I_{93.9}$ represent the measured peak intensities of $m/z = 95.9$, $m/z = 92.9$, $m/z = 91.9$, $m/z = 94.9$, and $m/z = 93.9$, respectively.
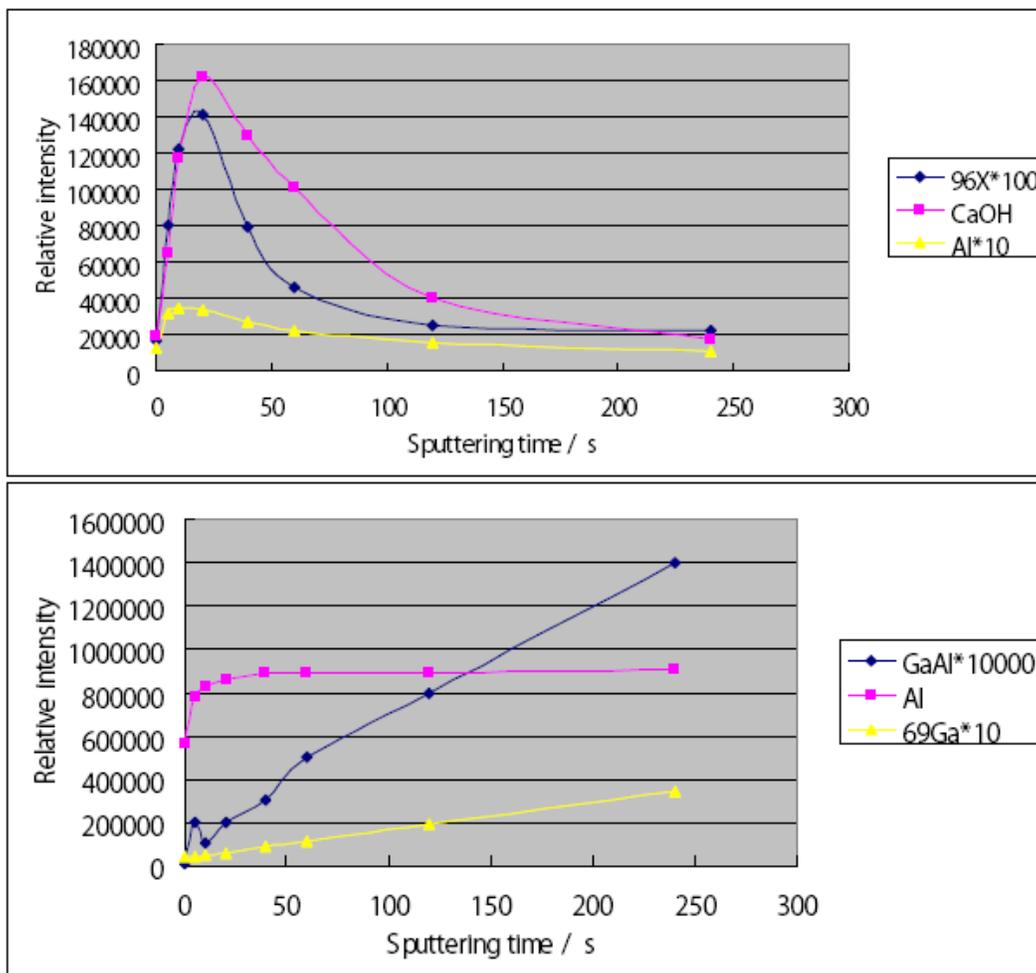
Figure 7. Depth profiles obtained by TOF-SIMS analysis; (a) ^{96}X+ (blue line), CaOH$^+$ (pink line), and Al$^+$ (yellow line) profiles for Sr implanted Pd/CaO multilayer after D$_2$ permeation; (b) GaAl$^+$ (blue line), Al$^+$ (pink line), and ^{69}Ga$^+$ (yellow line) profiles for Al foil.

On the other hand, theoretical intensity of $^{96}Mo^+$ (T_{96Mo}) can be calculated by a natural abundance ratio of ^{96}Mo to ^{92}Mo, i.e. (16.68/14.84) and measured peak intensity of $^{92}Mo^+$ as Eq. (2).

$$T_{96Mo} = (16.68/14.84)I_{91.9}. \tag{2}$$

Then, we define a deviation of measured intensity from theoretical intensity as Eq. (3).

$$D_{96Mo} = 100(I_{96Mo} - T_{96Mo})/I_{96Mo}. \tag{3}$$

When TOF-SIMS measurements were performed on eight different positions of a pure Mo metal plate, all the D_{96Mo} were within $\pm 4\%$. And when the measurements were performed with sputtering, the D_{96Mo} were approximately -5%, independently of sputtering time after 50 s as shown in Fig. 6. From above results, it was confirmed that the peak intensity of $^{96}Mo^+$ calculated with Eq. (1) is reliable within $\pm 5\%$ in the case of depth profiling, and that the intensity of $^{96}X^+$ can be calculated from the measured peak intensities of $m/z = 95.9$ and $m/z = 91.9$ as Eq. (4).

$$\begin{aligned} I_{96X} &= I_{95.9} - T_{96Mo} \\ &= I_{95.9} - (16.68/14.48)I_{91.9}. \end{aligned} \tag{4}$$

Figure 7 shows depth profiles of $^{96}X^+$ using the data calculated by the Eq. (4) with those of peaks relating to Ca_2O and GaAl. From Fig. 7(a), the profiles of $CaOH^+$ originating from CaO are rather similar to that of $^{96}X^+$. This result is compatible to the results of the investigation from accurate mass and isotope abundance. On the other hand, the profile of Al^+ is not so similar to that of $^{96}X^+$ as $CaOH^+$. Furthermore, from Fig. 7(b), the intensity of $GaAl^+$ is four orders of magnitude smaller than that of Al^+ at the surface after 120 s sputtering in the case of an Al foil, whereas the intensity of $^{96}X^+$ is only one order of magnitude smaller than that of Al^+ at 120 s sputtered surface. This result indicates that GaAl is negative as the candidate of ^{96}X.

From the above results of TOF-SIMS investigation, it was clarified that the peak of $m/z = 96$ observed on the sputtered surfaces is not $^{96}Mo^+$, $GaAl^+$ or $CaFe^+$, but Ca_2O^+ originated from Pd/CaO multilayer. This conclusion is supported by the fact that Ca_2O^+ is detected from surface region of a Pd/CaO multilayer not implanted with $^{88}Sr^+$ as shown in Fig. 8.

4. Conclusions

From the surface of the $^{88}Sr^+$ ion implanted Pd/CaO multilayer, Mo was clearly detected by XPS after D_2 permeation. However, this Mo was found to be a natural Mo from the isotope abundance obtained by TOF-SIMS.
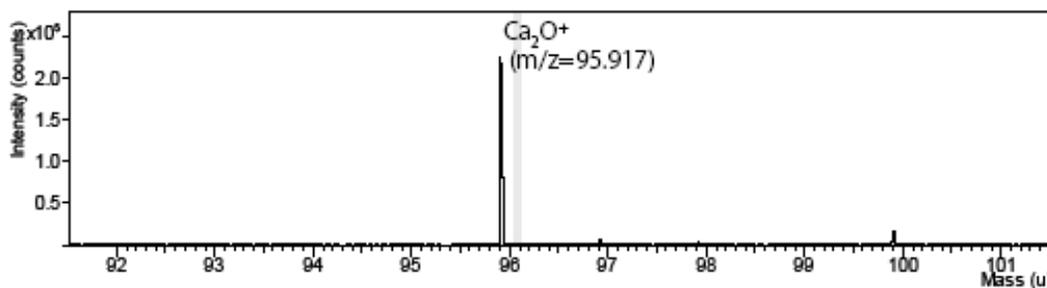
Figure 8. TOF-SIMS spectrum of Pd/CaO multilayer without Sr implanting. The integral of spectra from surface to about 5 nm depth by O_2 sputtering.

By TOF-SIMS analysis after removing the outermost surface layer containing natural Mo with ion sputtering, a strong peak at a mass close to ^{96}Mo was observed, which might be assigned to $GaAl^+$, Ca_2O^+ or $CaFe^+$, beside $^{96}Mo^+$.

By analyses of the TOF-SIMS data from the viewpoint of accurate masses, depth profiles and isotopic abundances, it was clarified that the peak of $m/z = 96$ was assigned to Ca_2O^+ originated from Pd/CaO multilayer.

Acknowledgments

References

[1] Y. Iwamura, M. Sakano, and T. Itoh, *Jpn. J. Appl. Phys.* **41** (2002) 4642–4648.
[2] T. Iwamura et al., *Proc. ICCF11*, Marseilles, France, 31 October–5 November, 2004, pp. 339–350.
[3] T. Higashiyama et al., *Proc. ICCF10*, Cambridge, USA, 24–29 August, 2003, pp. 447–454.
[4] A. Kitamura et al., *Proc. ICCF12*, Yokohama, Japan, 27 November–2 December, 2005, pp. 272–277.
[5] F. Celani et al., *Proc. ICCF10*, Cambridge, USA, 24–29 August, 2003, pp. 379–397.
[6] Y. Iwamura et al., *Proc. ICCF10*, Cambridge, USA, 24–29 August, 2003, pp. 435–446.
[7] T. Hioki, N. Takahashi and T. Motohiro, *Proc. ICCF13*, Sochi, Russia, June 25–July 1, 2007, Y. Bazhutov (Ed.), Publisher Center MATI, Moscow, Russia, 2008, pp. 518–528.
[8] J.S. Gao et al., *J. Vac. Sci. Technol.* **A28**(1) (2010) 147–151.
[9] T. Hioki et al., *Proc. ICCF14*, Washington DC, USA, 10–15 August, 2008, pp. 203–211.
[10] T. Hioki et al., *J. Condensed Matter Nucl. Sci.*, to be published.